

# Spatial Uncertainty Management for Simultaneous Localization and Mapping

Piotr Skrzypczyński

**Abstract**—In this paper we discuss methods to reduce spatial uncertainty in the simultaneous localization and mapping (SLAM) procedure for a mobile robot equipped with a 2D laser scanner and operating in a structured, but non-static environment. We augment the classic EKF-based SLAM procedure with two new modules. The first one reliably extracts line segments from the laser scans, employing a novel fuzzy-set-based grid map. The second one corrects the robot odometry by using scan matching. Both modules rely on a laser scanner measurement model, which covers both the quantitative and qualitative types of uncertainty.

## I. INTRODUCTION

Automated building of maps from sensory data is one of the central problems for autonomous robots. Many particular environment representations have been proposed in the literature [14]. A grid-based map can easily be updated with range sensors readings, tolerating data uncertainty and ambiguity, but requires a large amount of memory to cover bigger areas with a dense grid. In contrary, the feature-based map is a concise and explicit representation of the geometric entities. Such maps are less popular because of difficulties with the direct extraction of the features from raw sensory data. Whenever the robot pose  $\mathbf{x}_R = [x_r \ y_r \ \theta_r]^T$  is unknown, the map has to be constructed while computing a pose estimate. One of the most used methods to solve this SLAM problem is the Extended Kalman Filter (EKF), used with the feature-based maps [13]. Unfortunately, implementations of the EKF-based SLAM (hereinafter: EKF-SLAM) for robots operating in complicated indoor environments, that are often cluttered and populated, suffer from difficulties in the sensory data interpretation [4], [12] and limitations of the EKF framework [6].

To remedy these problems we propose a new approach to the geometric feature extraction from laser range data, that combines the advantages of both the feature-based and grid-based maps. A feature-based global map serves as representation of the environment in the EKF-SLAM. Horizontal straight line segments extracted from the 2D laser scanner data are used as features. These features can be further structured, representing distinctive objects in the environment [10].

A proper choice of the representation of geometric features has to be made, to avoid overparametrization and singularities, and to make the uncertainty independent of the used coordinates. To satisfy these requirements we have adopted the SPmodel feature representation [5].

P. Skrzypczyński is with the Institute of Control and Information Engineering, Poznań University of Technology, ul. Piotrowo 3A, PL-60-965 Poznań, Poland. ps@ar-kari.put.poznan.pl

The robustness to spurious and noisy range data exhibited by the grid-based maps stems mainly from the fact, that the given state of the particular cell is a result of many sensory readouts, taken at different moments and (typically) from different vantage points. These data are compared and integrated according to the chosen uncertainty calculus. In contrary, the features are usually extracted directly from the currently available laser sensor "snapshot", i.e. single scan. That makes this approach prone to errors due to spurious range measurements. The laser range measurements are affected by errors in the form of bias and noise [3]. Spurious readings are a result of a particular sensor behaviour, or are caused by dynamic objects in the vicinity of the robot.

To compensate this drawback of the feature-based map, we propose to use a local grid map, which supports the feature extraction by identifying the areas, that contain information on static objects (e.g. walls). The successively updated grid map accumulates data taken from several consecutive poses of the robot and filters out unreliable measurements.

By using two types of representation in parallel, we are also able to combine two frameworks for the uncertainty representation: the probabilistic methods to explicitly propagate quantitative uncertainty in the EKF-SLAM, and the fuzzy sets theory to remedy the qualitative-type uncertainty in the feature extraction.

## II. LASER SCANNER UNCERTAINTY MODEL

### A. Probabilistic Modelling of Uncertainty

The laser scanner on our Labmate robot is a Sick LMS 200. This sensor, which determines the distance by measuring the time of flight of the emitted pulse, is commonly applied on mobile robots for navigation. For the presented experiments it is configured to work in the 8 m range mode, with the angular resolution of  $0.5^\circ$ . In order to have a physical basis for the further error propagation and proper treatment of the spatial uncertainty in the feature extraction and SLAM we experimentally determined the main uncertainty components in the range measurements of the LMS 200 scanner. A more detailed characterization of the Sick LMS 200 sensor is provided by [16], however in this research a scanning mode with a different angular resolution was used.

Unlike the range data provided by older AMCW lasers [1], the bias of the LMS 200 scanner is to a large extent independent from the target surface colour and texture. The range bias was determined, and it was found that the bias is a function of both the measured distance  $r_m$  and the incidence angle  $\phi_i$  between the laser beam and the target

surface. However, we have found negligible the bias depending on the incidence angle for angles up to  $\phi_{i_{max}} = 70^\circ$ . Because the laser beam incidence angle is usually unknown while exploring an unknown environment, only a functional relationship between the bias and the measured range was established:

$$\begin{aligned} r &= r_m + \Delta r', \\ \Delta r' &= -16.8 + 5.8 \times 10^{-3} r_m - 6.7 \times 10^{-7} r_m^2, \end{aligned} \quad (1)$$

where  $r_m$  and  $r$  are the raw and the corrected range measurement, respectively. The equations (1) are used to correct (calibrate) the range measurements prior to their further processing.

An extensive set of experimental results involving different types and colours of surfaces ensured us, that the range measurement noise distribution is approximately Gaussian:

$$\hat{r} = \bar{r} + \delta r, \quad \delta r = N(0, \sigma_r), \quad (2)$$

where  $\bar{r}$  is a true (unknown) range, and  $\sigma_r$  is the range measurement standard deviation. The  $\sigma_r$  was found to be a slightly non-linear function of the measured range:

$$\sigma_r = 4.4 - 1.4 \times 10^{-4} r_m + 2.1 \times 10^{-7} r_m^2. \quad (3)$$

The uncertainty in the angle of the measurements is caused by the finite resolution of the scanner mirror encoder and the finite beam-width of the laser. However, in most of the laser scanners this uncertainty is very small, and it is often neglected [1]. We have determined the angular uncertainty, because it provides a physical basis for the sensor beam model required by the grid-based maps, and it is used by the scan matching algorithm [9] we have adopted. The angular uncertainty is also represented by a normal distribution:

$$\hat{\varphi} = \varphi + \delta\varphi, \quad \delta\varphi = N(0, \sigma_\varphi), \quad (4)$$

where the standard deviation  $\sigma_\varphi = 0.0083^\circ$  has been estimated taking into account the angular resolution of the scanner.

In Figure 1 a graphical interpretation of the LMS 200 scanner measurement uncertainty model is shown.

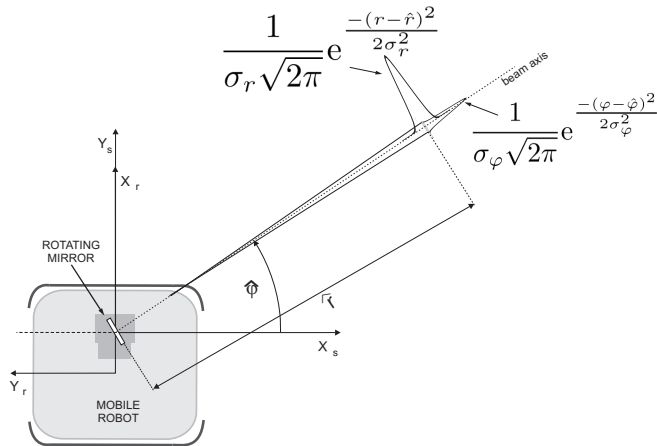


Fig. 1. The LMS 200 uncertainty model visualization

## B. Sources of Qualitative Errors

Besides the errors in the range measurements that can be described quantitatively and captured by a probabilistic model, such as the one we have proposed in the previous section, the laser scanners are prone to qualitative errors, which are caused by the interaction of the laser beam with particular objects in the environment. Such errors can be caused by mirror-like or pitch black surfaces, however the most common spurious range measurements arise when the laser beam hits simultaneously two surfaces at different distances. In a time of flight (TOF) scanner such a measurement appears between the two surfaces. This type of errors has been reported in many publications, for both AMCW [1] and TOF [15], [16] laser scanners, and is usually called "mixed pixels".

Because of the qualitative nature of the mixed pixels, there is no analytical model of the uncertainty caused by this phenomena. To avoid erratic behaviour of the map-building and localization procedures the mixed pixels should be eliminated at the early stage of feature extraction. However, there is no general method to recognize mixed pixels in the range measurements. The methods known from the literature are either sensor-specific [1] or application-specific [15]. Because of that, the EKF-SLAM should use a feature extraction procedure, which is robust to the mixed pixels, and other spurious measurements of similar nature, e.g. range readings corrupted by dynamic objects, such as people walking by the robot.

## III. GRID-ASSISTED FEATURE EXTRACTION

### A. Fuzzy Support Grid Concept

The grid maps handle the spatial uncertainty by estimating the confidence, that the given cell is empty or occupied. An important aspect of a grid map implementation is the mathematical framework used to represent and update this confidence. The most popular grid update scheme is based upon the Bayesian theory, which has well established foundations, but does not have ability to represent the lack of information. An alternative is the fuzzy-set-based method proposed in [8], which provides a good representation of different forms of uncertainty and incompleteness of information. In the previous research [11] we have found that the fuzzy grid map update scheme is most appropriate for the application under study, being able to filter out corrupted measurements caused by dynamic objects in the vicinity of the robot, and most of the mixed pixels.

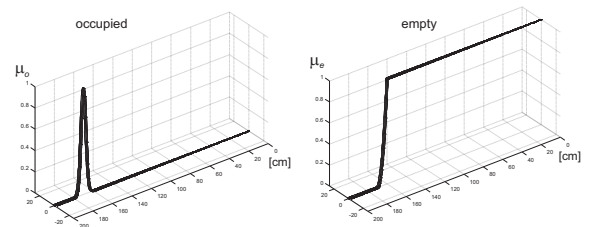


Fig. 2. Membership functions for the LMS 200 laser beam

In the fuzzy-set-based mapping method, originally developed for a sonar-equipped robot, the sets of occupied  $\mathcal{O}_i^k$  and empty  $\mathcal{E}_i^k$  cells are determined by computing their membership functions according to the sensor beam model (Fig. 2) for every  $i$ -th range measurement taken from the  $k$ -th robot pose. In our implementation, the sensor model represents the degrees of membership of a given cell to the sets of occupied and empty cells, according to the laser range reading  $r$ , and its uncertainty  $\sigma_r$  [11]. The data gathered from a single robot pose are aggregated to the sets  $\mathcal{O}^k$  and  $\mathcal{E}^k$ , representing locally the occupied and empty cells, respectively. The sets  $\mathcal{E}^k$  and  $\mathcal{O}^k$  generated at the  $k$ -th pose are aggregated with the previously available information. Two sets describing the lack of information, by identifying the cells being ambiguous ( $\mathcal{A}$ ) or indeterminate ( $\mathcal{I}$ ) are computed:

$$\mathcal{O} = \mathcal{O} \cup \mathcal{O}^k, \quad \mathcal{E} = \mathcal{E} \cup \mathcal{E}^k, \quad \mathcal{A} = \mathcal{E} \cap \mathcal{O}, \quad \mathcal{I} = \bar{\mathcal{E}} \cap \bar{\mathcal{O}}. \quad (5)$$

Because our aim is to build a feature-based model of the environment, we are looking for cells providing reliable support for line segment extraction. To this end, we define a set of *support* cells, being very occupied and unambiguous. The term "very occupied" emphasizes the difference between low and high values of occupancy, and is implemented by squaring the value of the membership function:

$$\mathcal{S} = \mathcal{O}^2 \cap \bar{\mathcal{A}} \cap \bar{\mathcal{I}}. \quad (6)$$

In the local fuzzy support grid (FSG) computed according to (6) the contours of objects are identified as aligned cells of high membership degree to the  $\mathcal{S}$  set. Figure 3 shows a 3D view of a FSG map resulting from an experiment with the LMS 200 scanner, where the higher values mean better support for line extraction, while the darker peaks are the spurious measurements, mostly due to people walking by or small obstacles moved during the experiment.

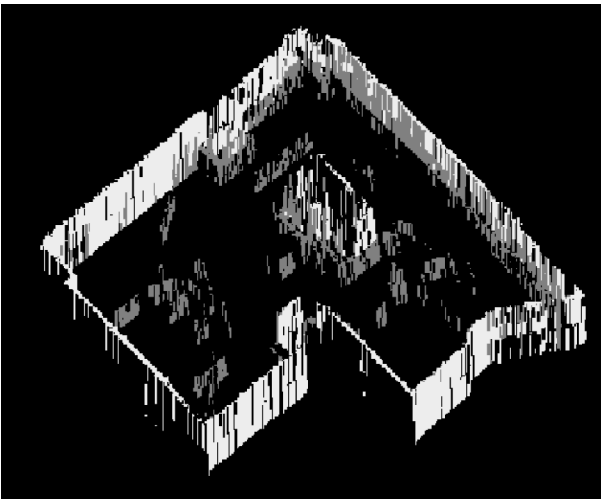


Fig. 3. An example of the fuzzy support grid

Unlike the feature-based map, the grid-based mapping paradigm provides no means to accommodate the spatial

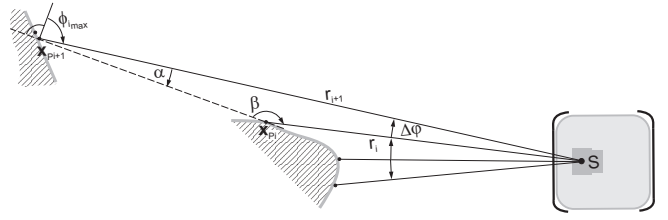


Fig. 4. Maximum measured distance in the clustering algorithm

uncertainty induced by pose errors. Because of that, if the FSG is built using scans registered with the odometry, it can become inconsistent due to registration errors. To reduce such problems, we correct the odometry with the estimates of relative robot displacement obtained from incremental scan matching [12].

### B. Feature Extraction Method

There are several known approaches to the extraction of lines from a grid-type representation. One of the most used is the Hough transform [9], [11]. Unfortunately, the Hough transform does not take the spatial uncertainty into account when estimating the line parameters, and introduces itself an uncertainty depending on the level of discretization of the parameter space. The loss of precision is also inherent to the grid representation, because individual range readings are incorporated into the cells of given size, hence the information about their precise position is lost.

An alternative are the scan splitting algorithms that consider the order in which the range measurements were obtained. Such an algorithm is the Iterative End Point Fit (IEPF), which we have already used in the previous work [10]. This "divide and conquer" type algorithm is much faster than the Hough transform. However, the order of range measurements scanned from a particular robot pose is not preserved in the grid map. Because of that, the proposed segment extraction method considers individual scans instead of the whole fuzzy grid, while the FSG is used to judge the validity of the individual measurements, by comparing them to the evidence accumulated by the past scanner readings.

The line segments are extracted from the ordered set of laser scanner points. Only the points, that fall in the FSG cells of high membership degree to the  $\mathcal{S}$  set are considered in further processing. The spatial uncertainty of a point is represented by its covariance matrix computed upon the values of  $\sigma_r$  and  $\sigma_\varphi$  obtained from the laser scanner uncertainty model.

The points are grouped together to form individual objects. This procedure should reliably find all discontinuities in a scanned sequence of points. A tracking-like, EKF-based approach to the detection of discontinuities has been proposed in [5]. The process model used in this approach does not have any physical basis, what makes it's parameter values hard to tune. The procedure is also computationally expensive, due to the Mahalanobis distance computation required for each measurement.

Starting from the analysis of the LMS 200 sensor qualitative uncertainty, we have developed a different approach, which is computationally efficient and based on the underlying physics of the laser range measurements. We have observed, that the incidence angle  $\phi_i$  for each valid measurement must be smaller than the experimentally found  $\phi_{i_{max}}$ . If the previous measured range  $r_i$  is known, then from this value, and the scanner angular resolution  $\Delta\varphi$  one can compute the maximum and minimum values of the next range  $r_{i+1}$ , that satisfy the criteria  $\phi_{i_{r_{i+1}}} \leq \phi_{i_{max}}$  (Fig. 4). If the actual measured range falls between these values, then it is accepted as a member of the same group as its predecessor. If not, the measurement is treated as a beginning of a new group. The following pseudo-code shows this algorithm:

```

procedure RANGECLUSTERING( $n_p, \phi_{i_{max}}, \Delta\varphi$ )
   $k_{min} := \frac{\cos(\phi_{i_{max}} + \Delta\varphi)}{\cos \phi_{i_{max}}}$  ; {min. range factor}
   $k_{max} := \frac{\cos(\phi_{i_{max}} - \Delta\varphi)}{\cos \phi_{i_{max}}}$  ; {max. range factor}
   $n_g := 1$  ; {group counter initialised}
   $n_g(r_1) := n_g$ ;
  for  $i := 1$  to  $n_p - 1$  do
    if  $r_{i+1} > (r_i k_{min} - 3\sigma_r)$  and  $r_{i+1} < (r_i k_{max} + 3\sigma_r)$ 
      then  $n_g(r_{i+1}) := n_g$ 
    else  $n_g := n_g + 1$ ;  $n_g(r_{i+1}) := n_g$  {new group}
  return  $n_g$ . {returns all groups}

```

In this algorithm  $n_p$  is the number of points in the scan,  $n_g$  is a group number of a given measurement,  $\sigma_r$  is the measurement standard deviation obtained from (3). If the number of points in a group is small, then this group is discarded as containing outliers. An approach to laser scanner data clustering, which is based on an idea similar to the one used in the above-presented algorithm has been discussed in [4]. However, the method of [4] works in the Cartesian coordinates, what makes it computationally less effective.

Next, the IEPF algorithm is applied to find candidate line segments from groups of points representing particular objects. The supporting line of an extracted segment is described by the SPmodel feature  $L_{RF}$ , with regard to the robot frame. The feature parameters and covariance are computed by applying the weighted total least squares method. The endpoints of the segment are determined by projecting the laser points onto the infinite line and trimming the line at the extreme points. Finally, the center point and the length  $l_F$  are computed. There is no uncertainty of the segment length determined.

Results obtained with the FSG-supported segment extraction method have been compared in Fig. 5 to the results of the standard split-and-merge approach to laser data segmentation [5]. When a scan (Fig. 5A) containing range measurements caused by a dynamic object (indicated by "1") and some outliers due to mixed pixels ("2") is processed by the IEPF algorithm, the resulting local map (Fig. 5B) contains artifacts and segments, whose orientation is poorly estimated. If the segmentation is assisted by the FSG map (Fig. 5C), which identifies the areas, that provide reliable support for line segment extraction, the resulting local map (Fig. 5D) is

better. It does not contain artifacts related to dynamic objects. The remaining line segments have more correct location, because the FSG filtered out vast majority of the outliers, that in the standard approach acted as "leverage points" during the least squares estimation of supporting lines parameters.

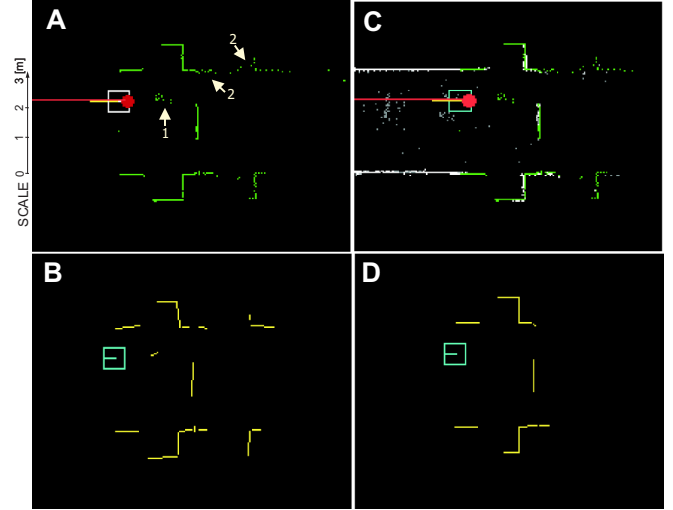


Fig. 5. Comparison of line segment extraction results: without and with the FSG

The FSG map is built at the full scan rate. The geometric features (segments) are extracted in average each ten FSG updating cycles. The scanned points that are acquired between two consecutive calls to the feature extraction procedure contribute to the FSG map, so the evidence they carry as to the occupancy of particular areas supports the feature extraction process.

#### IV. SIMULTANEOUS LOCALIZATION AND MAPPING

The mobile robot builds the global, feature-based map simultaneously while localizing within it. The EKF-SLAM algorithm with the stochastic map [13] is implemented, therefore the map is represented by the state vector  $\hat{x}$  containing the estimated pose of the robot  $\hat{x}_R$  and the estimated locations of  $n$  features  $\hat{x}_{WF_i}$ , ( $i = 1 \dots n$ ). The spatial uncertainty of the estimated features, the robot pose, and their correlations are represented by the covariance matrix  $C_x$ . All locations are represented with regard to the global reference frame  $W$ . The initial robot pose is used as the base coordinates.

In the EKF-SLAM prediction stage, the state vector at the  $k$ -th step is computed by estimating the robot relative displacement from  $k-1$  to  $k$ . In wheeled robots the displacement estimate is provided by the encoder-based odometry. However, if the residual systematic errors in the odometry are significant, or the random error isn't modelled correctly, the pose uncertainty, particularly in the orientation, easily lead to EKF divergence [6]. Because some odometry errors cannot be anticipated by any mathematical model, one must recourse to other types of sensors to improve the robot displacement prediction. If proprioceptive sensors such as rate-gyros and

compasses [3] are not available, the displacement estimate can be obtained from an exteroceptive sensor.

In the SLAM framework, the uncertainty in both the robot pose and the feature locations is decreased by re-observing the features. The new observations are the segments in the current local map. They are extracted from the laser scanner data according to the approach presented in the previous section. The observations are matched with the features stored in the global map. The successfully associated features are used to update the state vector and its covariance by applying the well-known EKF equations. Unmatched features from the local map are added to the global map, augmenting the state vector.

The computational complexity of the EKF-SLAM estimation stage is  $O(n^2m)$ , where  $m$  is the number of matched features [5]. If the feature matching fails, e.g. due to spurious features, the global map grows quickly, what makes the estimation time unacceptable and prohibits on-line operation of the robot.

## V. ROBOT DISPLACEMENT ESTIMATION

Keeping track on the robot pose and its uncertainty during motion of the vehicle is important to both the FSG-assisted feature extraction and the EKF-SLAM itself. The encoder-based odometry alone is insufficient to accomplish this task, because of undetected bias and uncertainty due to unforeseen or "catastrophic" errors [3].

One approach to overcome these problems is to employ the laser scanner readings to estimate the relative displacement between two sequential steps of the EKF-SLAM. The relative translation and rotation between two robot poses can be obtained by scan matching, i.e. by finding a rotation and translation that maximize the overlap of these scans. For correction of the odometry errors we match two consecutive scans to compute the incremental displacement  $\Delta \mathbf{x}_{R_i}$ . Integrating these displacements, given by the translation  $\Delta \mathbf{t}_i = [\Delta x_i \ \Delta y_i]^T$  and rotation  $\Delta \theta_i$  for the pair of scans  $i - 1$  and  $i$ , we establish an alternative form of odometry.

There are a number of methods for matching scans known from the literature. Unfortunately, most of these methods do not provide a realistic covariance matrix  $\mathbf{C}_\Delta$  of the relative displacement estimate [2]. Such an estimate is required to integrate the alternative odometry measurements in the prediction stage of the EKF-SLAM algorithm. One of the scan matching methods, that satisfy this requirement is the WLSM algorithm presented in [9]. The WLSM algorithm explicitly models the sources of errors in both the range measurements and the matching process itself, hence it is able to calculate a realistic covariance of the displacement. We have implemented this algorithm as the basis for the alternative odometry.

A key assumption underlying the use of Kalman filtering in the SLAM algorithm is that the robot motion estimate is statistically independent from the exteroceptive observations. Due to this reason we cannot use for scan matching the same range data, which are then used for the feature extraction. As already mentioned, the points from only one scan per ten

are used for the line segment extraction, with the remaining laser data updating only the FSG membership values. Our alternative odometry adheres to this data processing scheme, by using only the scans taken in-between two consecutive steps of the EKF-SLAM algorithm [12]. This way separate range readings are used to estimate the vehicle motion and the features, what ensures independence of the information sources in the Kalman filter.

## VI. EXPERIMENTAL RESULTS

In order to verify the presented approach to the spatial uncertainty management, we have performed several experiments with the Labmate robot equipped with the LMS 200 scanner.

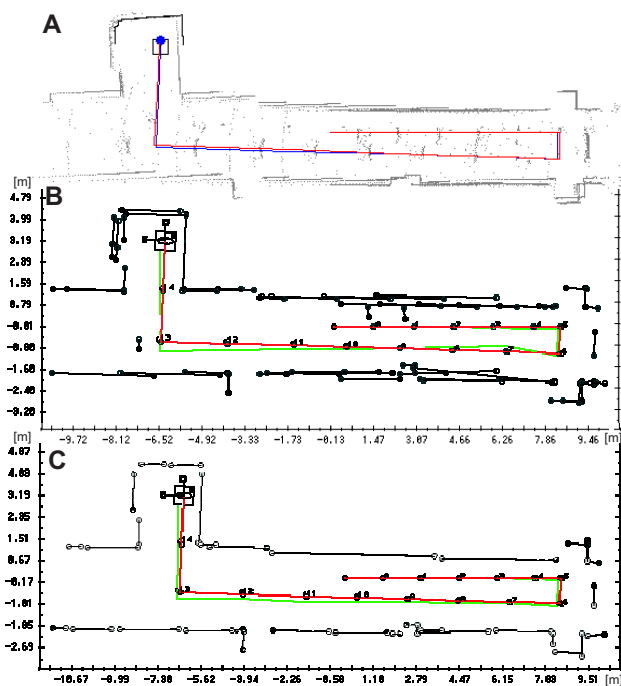


Fig. 6. Maps resulting from an experiment in the corridor

Figure 6 shows how filtering of dynamic objects and outliers improves quality of the segment-based map. In Fig. 6B a map built by the SLAM algorithm from the raw data shown in Fig. 6A is depicted. It contains a number of spurious segments in the areas where the scan points caused by a dynamic object (a person walking in front of the robot) were encountered. The green line indicates the estimated robot path, while the red line is for the odometry. A map created by the SLAM algorithm using the FSG-supported feature extraction and improved motion estimates is shown in Fig. 6C. This map contains fewer line segments and there are no segments resulting from the dynamic object.

Figure 7 shows results of an experiment, in which parameters of the Labmate odometry model have been roughly identified by an ad-hoc experiment, leaving the systematic errors not calibrated. The first map was built with the basic EKF-SLAM algorithm, without use of the FSG and scan matching. As it can be seen from Fig. 7A it contains many

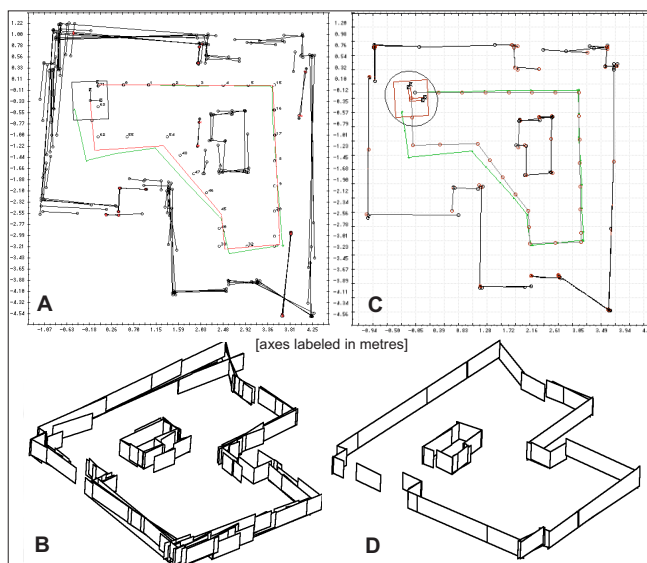


Fig. 7. Comparison of results for the experiment with poor odometry: standard EKF-SLAM (A,B) and the improved system (C,D)

overlapping segments and is highly inconsistent. Divergence of the EKF due to the not calibrated systematic component, and inaccuracies in the model of the non-systematic odometry errors gradually prevented correct associations between the map and the segments from new observations, as shown by the plot of successful feature matching ratio in Fig. 8A. The segment-based map obtained from the scanner data gathered with the same experimental set-up, but using the proposed framework (Fig. 7C) is much more consistent. The estimates of robot displacement obtained from local scan matching prevented the EKF from large divergence in spite of the poorly modeled vehicle odometry. The ratio of feature matching is higher (Fig. 8A). Some segments are still multiplied, but the overall number of features in the second map is greatly reduced. The improvement in the quality and geometric consistency of the resulting global map can be best seen on the 3D views (Fig. 7B and Fig. 7D). Reduction of the spurious features alleviates computational burden in the EKF-SLAM algorithm, what is shown by the plot of the map estimation time (Fig. 8B).

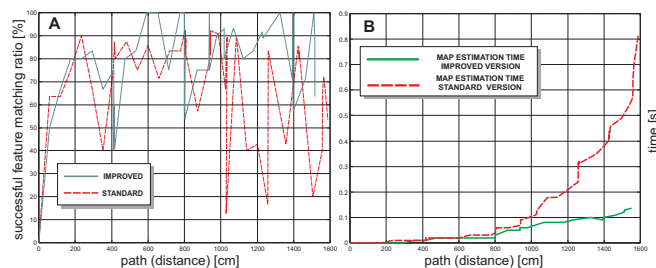


Fig. 8. Successful matchings (A) and estimation time (B)

## VII. CONCLUSION

We have proposed a new approach to the spatial uncertainty management in the feature-based EKF-SLAM for an

indoor mobile robot. The types and sources of the uncertainty, that are most devastating to the EKF-SLAM performance have been identified. To compensate this uncertainty, new data processing modules have been introduced to the SLAM procedure. The feature extraction module benefits from using simultaneously both the grid-based and feature-based mapping paradigms, that are usually used separately, and often are contrasted in the literature [14]. The relative displacement estimation module employs local scan matching. This procedure is used by many researchers as an incremental self-localization method on its own, and was combined with a particle-filter-based SLAM solution [7] in a way similar to our idea of the alternative odometry. However, we have shown experimentally, that the scan matching with a physically-grounded uncertainty model improves also the EKF-SLAM enabling better pose prediction, what in turn reduces the linearization errors and wrong feature associations.

## REFERENCES

- [1] M. D. Adams, *Sensor Modelling, Design and Data Processing for Autonomous Navigation*, Singapore, World Scientific, 1999.
- [2] O. Bengtsson, A.-J. Baerveldt, "Localization by Matching of Range Scans – Certain or Uncertain", *Eur. Works. on Advanced Mobile Robots (Eurobot'01)*, Lund, 2001.
- [3] J. Borenstein, L. Feng, "Measurement and Correction of Systematic Odometry Errors in Mobile Robots", *IEEE Trans. Robot. & Autom.*, 12(6), 1996, pp. 869-880.
- [4] G. A. Borges, M.-J. Aldon, "Line Extraction in 2D Range Images for Mobile Robotics". *Journal of Intelligent and Robotic Systems*, 40, 2004, pp. 267-297.
- [5] J. A. Castellanos, J. D. Tardós, *Mobile Robot Localization and Map Building. A Multisensor Fusion Approach*, Boston, Kluwer, 1999.
- [6] J. A. Castellanos, J. Neira, J. D. Tardós, "Limits to the Consistency of the EKF-based SLAM", *Prepr. IFAC Symp. on Intell. Autonomous Vehicles*, Lisbon, 2004, CD-ROM.
- [7] D. Hähnel, W. Burgard, D. Fox, S. Thrun, "An Efficient FastSLAM Algorithm for Generating Maps of Large-Scale Cyclic Environments from Raw Laser Range Measurements", *Proc. IEEE/RSJ Conf. on Intell. Robots & Syst.*, Las Vegas, 2003, pp. 206-211.
- [8] G. Oriolo, G. Ulivi, M. Venditelli, "Real-time Map Building and Navigation for Autonomous Robots in Unknown Environments", *IEEE Trans. Syst., Man & Cybern.*, Part B, 28(3), 1998, pp. 61-70.
- [9] S. Pfister, K. Kriechbaum, S. Roumeliotis, J. Burdick, "Weighted Range Sensor Matching Algorithms for Mobile Robot Displacement Estimation", *Proc. IEEE Int. Conf. Robot. & Autom.*, Washington, 2002, pp. 1667-1674.
- [10] P. Skrzypczyński, "Environment Modelling Using Optical Scanner Data", *Proc. IFAC Symp. on Robot Control*, Nantes, 1997, pp. 187-192.
- [11] P. Skrzypczyński, "Merging Probabilistic and Fuzzy Frameworks for Uncertain Spatial Knowledge Modelling", *Computer Recognition Systems*, M. Kurzyński et al., (eds.), Berlin, Springer, 2005, pp. 435-442.
- [12] P. Skrzypczyński, "Laser-based Logical Sensors for Improved Mapping and Localization", *Proc. Eur. Conf. on Mobile Robots*, Ancona, 2005, pp. 50-55.
- [13] R. Smith, M. Self, P. Cheeseman, "Estimating Uncertain Spatial Relationships in Robotics", *Autonomous Robot Vehicles*, I. Cox, G. Wilfong, (eds.), Berlin, Springer, 1990, pp. 167-193.
- [14] S. Thrun, *Robotic mapping: a survey*, Tech. Rep., CMU-CS-02-111, 2002.
- [15] J. Tuley, N. Vandapel, M. Hebert, "Analysis and Removal of Artifacts in 3-D LADAR Data", *Proc. IEEE Int. Conf. Robot. & Autom.*, Barcelona, 2005, pp. 2203-2210.
- [16] C. Ye, J. Borenstein, "Characterization of a 2-D Laser Scanner for Mobile Robot Obstacle Negotiation", *Proc. IEEE Int. Conf. Robot. & Autom.*, Washington, 2002, pp. 2512-2518.